A closer look at CT scanning

Author : Charissa Lee, Natalie Webster

Categories : General, Vets

Date : April 3, 2017

A basic CT unit consists of a gantry containing an x-ray source and x-ray detector system, a patient table and an operator console.

Patients are positioned on the table, in the centre of the gantry. The horizontal plane (patient width) is described as the x-axis and the vertical plane (patient height) described as y-axis. There is also a third dimension – the z-axis – along the length of the patient table.

Image acquisition and reconstruction

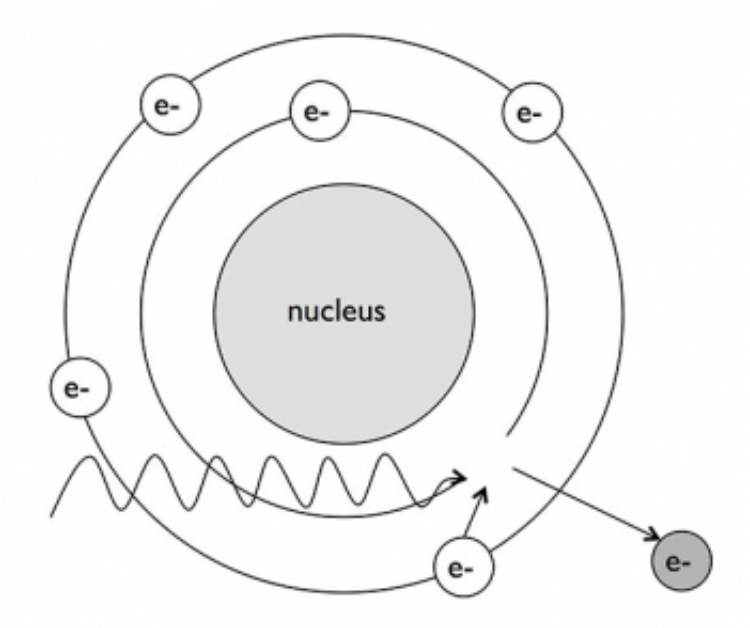

Figure 1. The photoelectric effect. The x-ray ejects an electron from the inner shell and is completely absorbed. An electron from the outer shell fills the position and the ejected photoelectron produces ionisations in the tissue.

As x-ray beams pass through the patient, energy is attenuated. The amount of attenuation depends on the type of tissue, as dictated by two main mechanisms: photoelectric effect (**Figure 1**) and Compton scattering (**Figure 2**)[1].

Unlike radiographs, where attenuation is qualitative, attenuation in CT is quantitative. The detector measures the attenuation – the fraction of radiation removed along the path of the x-ray beam through the patient.

However, to differentiate the attenuation of tissues along the way, a set of projections is required, and a mathematical process called filtered back projection is applied. This allows mean attenuation values to be given to each small cubical section along the path of the x-ray beam. These small cubical sections, also known as voxels, together make a thin slice of the body. The attenuation values for each voxel are then transformed into Hounsfield units (HU) or CT numbers, and normalised to a reference material, such as water (CT number 0)[2,3].

Each voxel corresponds to a pixel in the CT image and the CT number for it is represented as a shade of grey – thus giving a map of the distribution of tissue types within a slice. As CT numbers from scanners range from about ?1,000 to +3,000, more than 4,000 shades of grey need to be displayed. However, we can generally only discern around 30 shades[4].

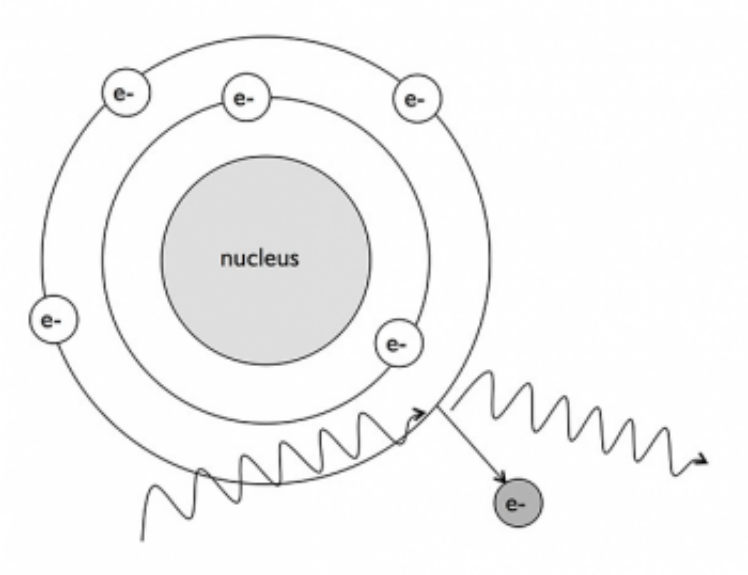

Figure 2. Compton scattering. The incoming x-ray ejects an electron from the outer shell and is scattered rather than absorbed. The ejected photoelectron produces further ionisations in the tissue and is eventually absorbed by the patient.

Furthermore, as many soft tissue numbers fall within a narrow part of the range between air and bone (**Table 1**), by evenly spreading out the full CT number range over discernible grey levels, many of these structures would have the same level of grey as their surroundings. To counteract this problem, the technique of windowing can be performed, whereby window width is the range of CT numbers to display and window level is defined as the mid-point in that range. CT numbers above and below that range would be set to white and black respectively[2,4].

CT scanners

In first generation scanners, the x-ray tube and detector are both locked in relative position and orientation, and x-rays are filtered and collimated to produce a pencil beam (**Figure 3**).

Acquisition of a single slice involved translating the tube and detector across the patient width-wise, rotating a degree and repeating the same process until 180° of data is obtained. This is known as a translate-rotate system. However, the time taken to obtain a single slice was approximately four to five minutes. Thus, first generation scanners are not commonly used in clinical practice[2,4].

Second generation scanners have both the x-ray tube and detectors locked in relative position. However, instead of a pencil beam, a fan beam was used, and the number of detectors on the other side of the patient was increased (**Figure 4**).

Second generation scanners are known as multidetector translate-rotate systems. Compared with first generation scanners, scan times could be reduced to as low as 20 seconds, but, due to the use of multiple detectors, scatter radiation was more pronounced, even with the use of grids and collimators[4].

Third generation scanners are the basis for most CT scanners at present. In these scanners, although the x-ray tube and detectors are locked in relative position, the fan beam is sufficiently wide enough to cover the whole cross section of the patient (**Figure 5**). To acquire a slice, the tube and detector rotate 360° around the patient to obtain data.

Third generation scanners are known as rotate-rotate type systems. Without the need for translational motions, scan times became as low as 0.5 seconds[4,5]. Detectors in fourth generation scanners are placed in a 360° stationary ring and only the x-ray tube rotates, making it a fixed-rotate system (**Figure 6**). Image acquisition is achieved by the collection of a complete fan beam view by one detector. In other words, data measured by one detector as the x-ray tube rotates is similar to one third generation fan beam view[2].

However, due to the high costs associated with having many detectors, and the large size of the unit, fourth generation CT scanners are not often used for multislice CT units[5].

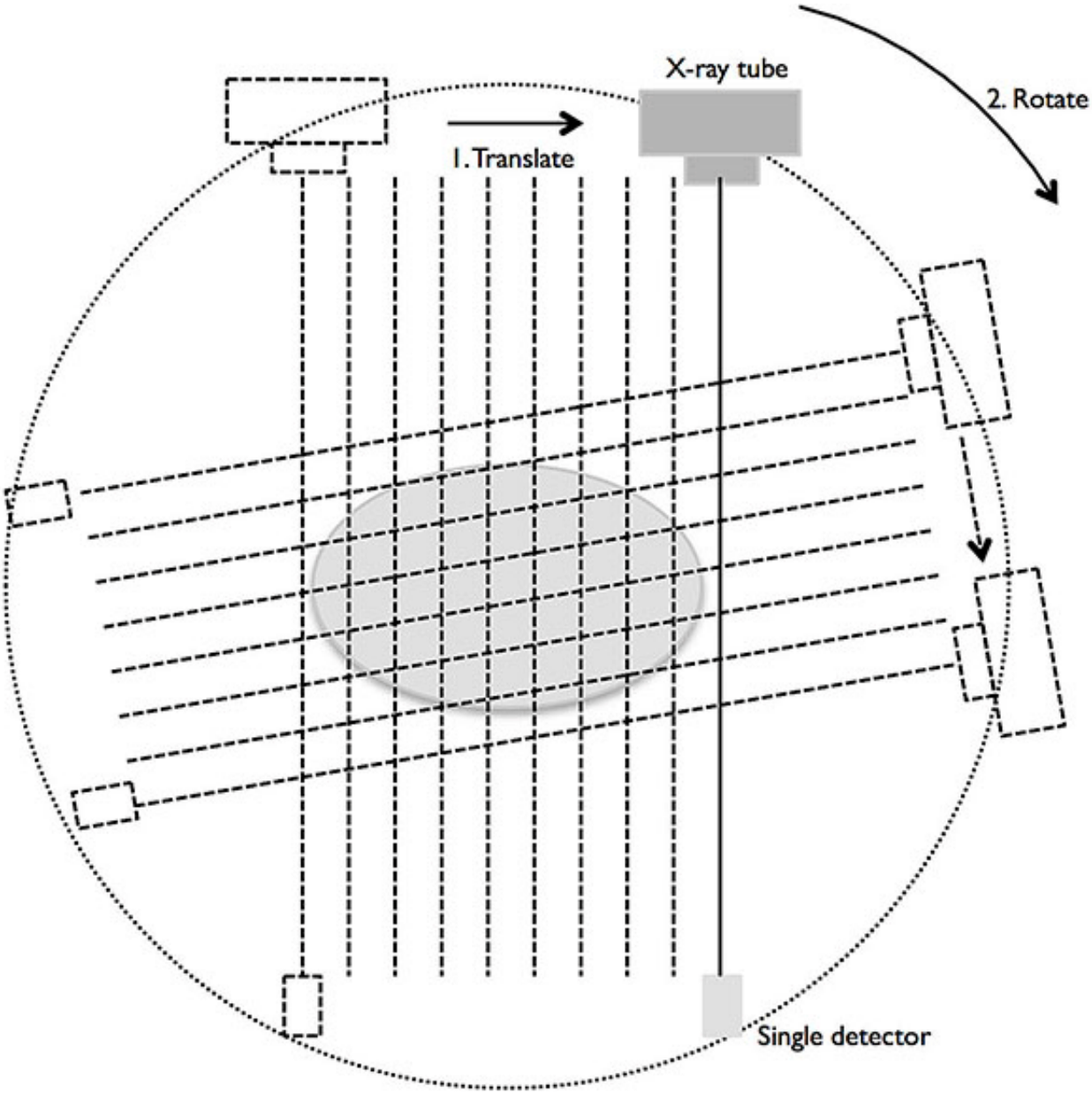

Figure 3. First generation CT scanner geometry.

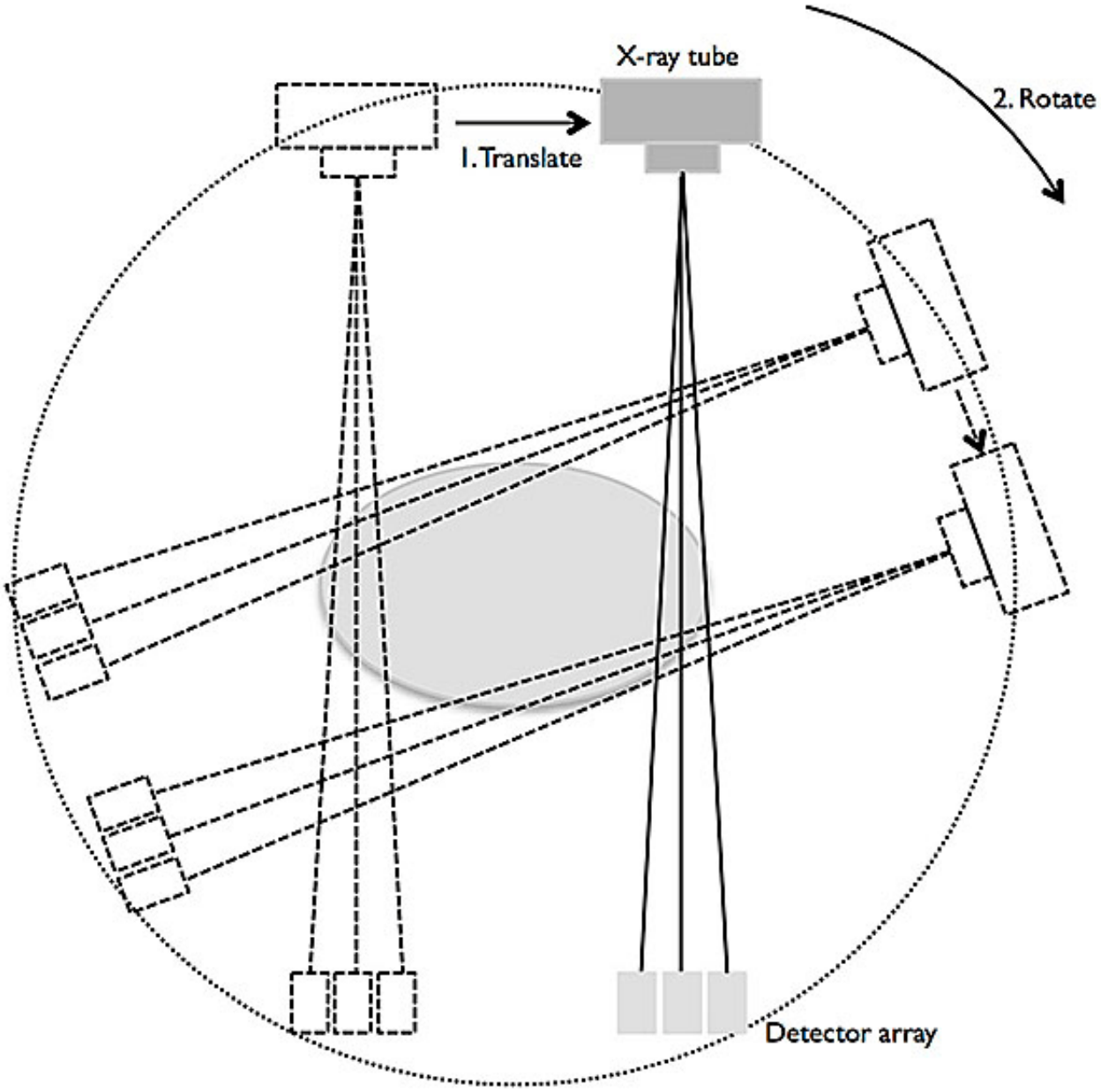

Figure 4. Second generation CT scanner geometry.

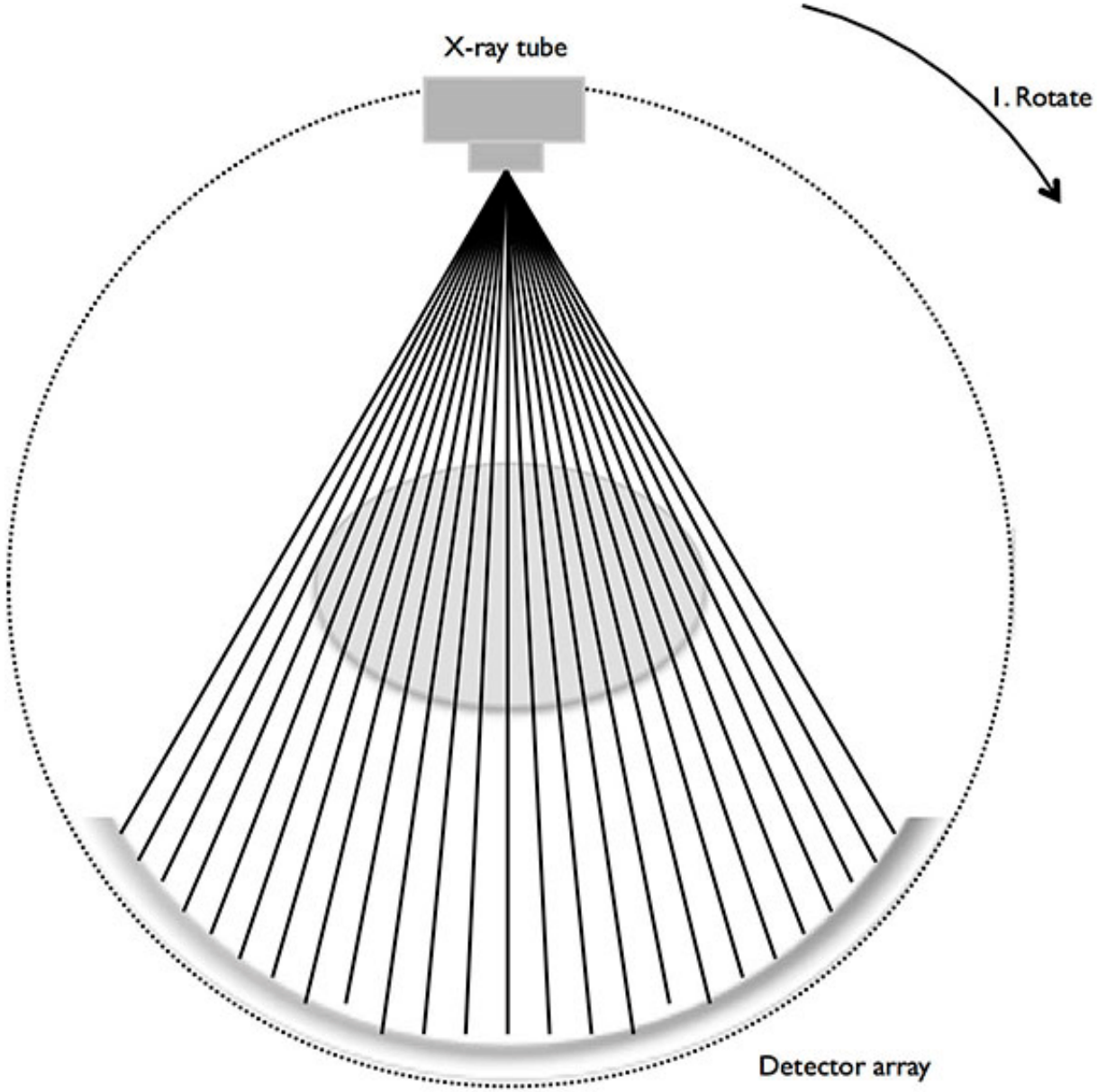

Figure 5. Third generation CT scanner geometry.

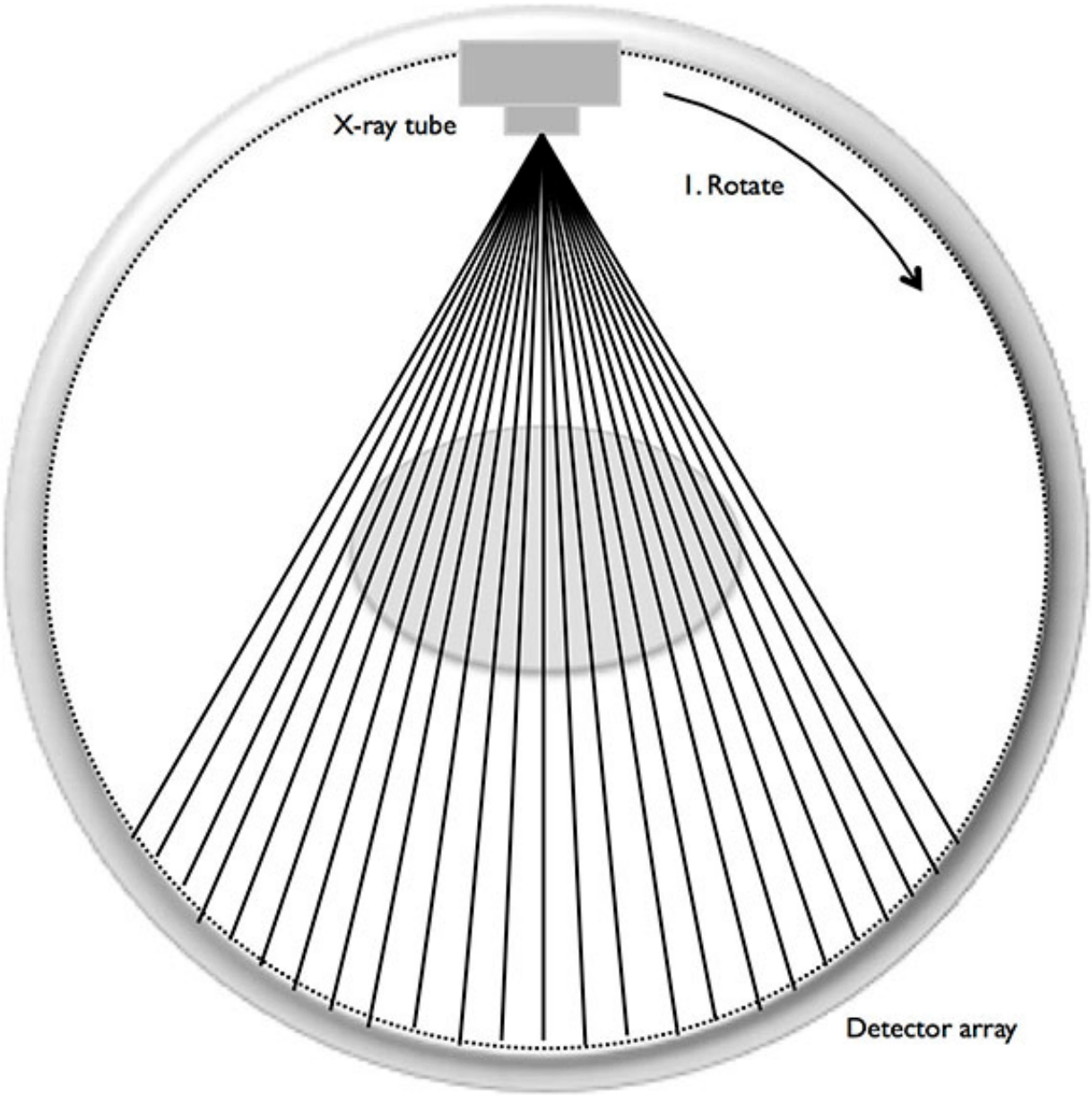

Figure 6. Fourth generation CT scanner geometry.

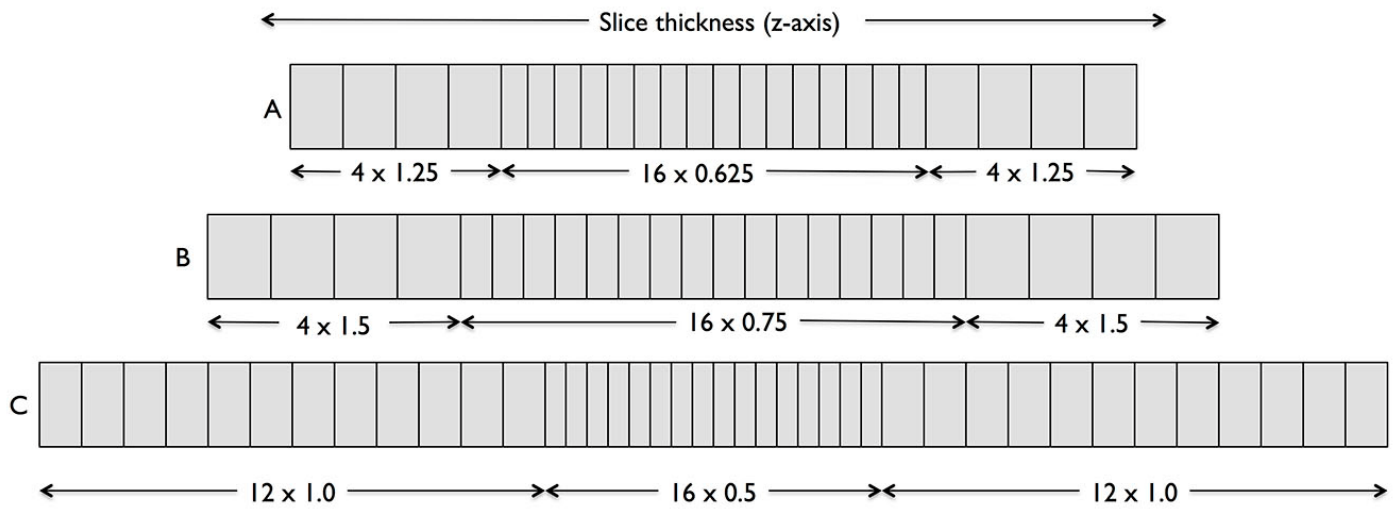

Figure 7. Designs of various 16-slice detector systems. Inner detectors can collect 16 thin slices or be combined to collect thicker slices. A = GE Healthcare, B = Philips and Siemens, C = Toshiba.

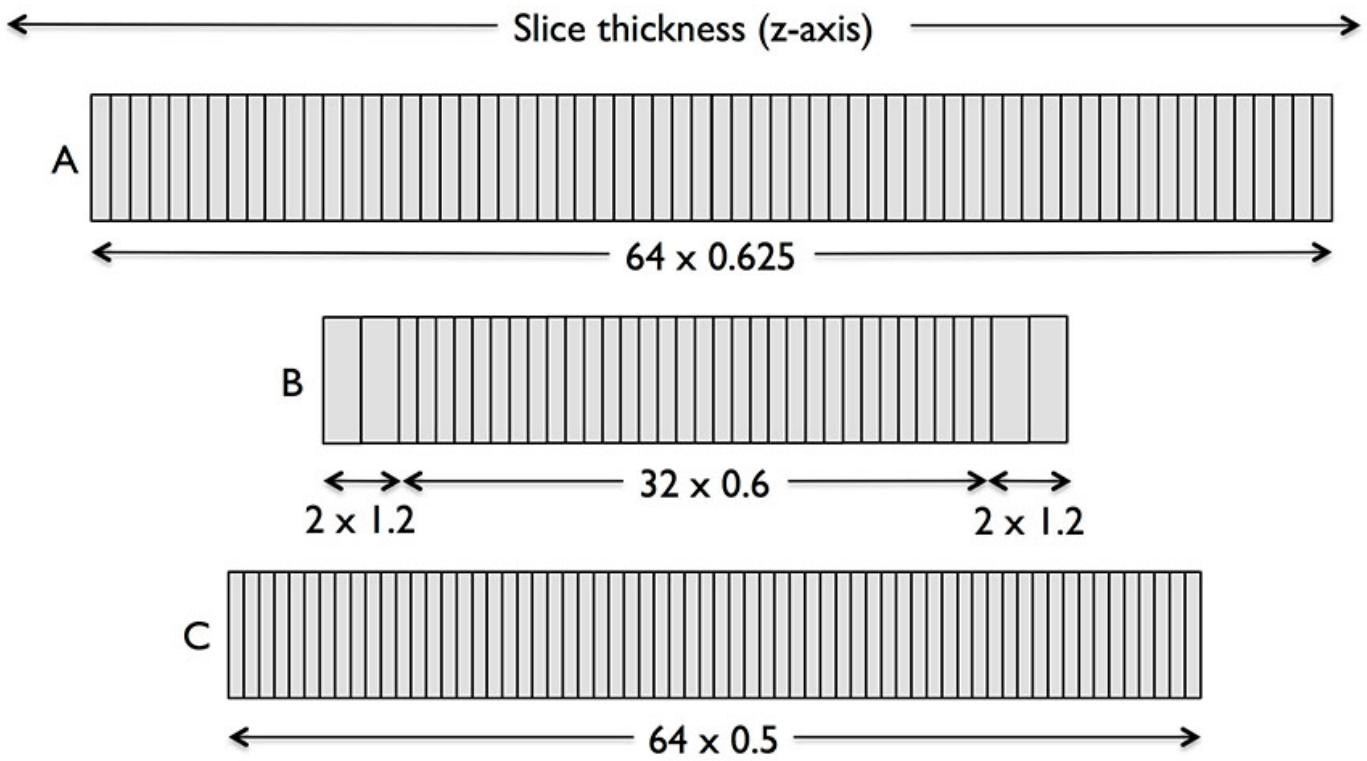

Figure 8. Designs of various 64-slice detector systems. A = GE Healthcare and Philips, B = Siemens, C = Toshiba.

Slip ring scanners

Table 1. Typical CT number values[4]

Tissue type	CT number
Air	−1,000
Fat	−60
Water	0
Cerebrospinal fluid	10
Brain white matter	30
Brain grey matter	38
Blood	42
Muscle	44
Haemorrhage	80
Dense bone	~1,000

Table 1. Typical CT number values[4].

The development of slip ring scanners came about following the need to reduce interscan times. In previous rotational scanners, due to electrical components such as cables, the scanners needed to stop after 360° and reverse direction before taking another slice.

Using electrical brushes, slip ring technology allows electrical power to pass to the rotating components from stationary components. This results in continuous circular rotation of the rotating components, thus reducing interscan times. However, delays existed from having to move the table to the next slice position after each scan[2].

Helical and multislice CT

Helical CT is the alternative to the axial step-and-shoot CT (scan-move-scan sequence). It uses slip ring technology for continuous tube and detector rotation, as well as continuous translation of the table through the gantry, allowing data to be acquired continuously. The result is an x-ray tube that takes a helical path relative to the patient, and a huge reduction in the time taken to scan a region of interest[2,5].

Though total scan times became shorter, tube heating became a problem[6]. To address this, x-ray tubes were made with higher heat capacity and the idea of multislice CT was developed.

In multislice CT, the x-ray beam is widened in the z-direction and multiple rows of detectors are added. This effectively allows for more coverage with each rotation, as well as reduces the total usage of the x-ray tube[6]. With scanning times reduced, better contrast resolution can be obtained with less motion artefacts[5].

Multislice detector systems are available in a range of designs, including 16-slice and 64-slice detectors (**Figures 7 and 8**)[6]. The sizes of the detectors determine the smallest possible slice thickness, while the collimators determine how many detectors are used. Detectors can also be combined in a process called binning, allowing for variations in slice thickness. Detector array designs can either have detectors with equal widths or detectors with unequal widths[5].

CT scan modes

Scout scan

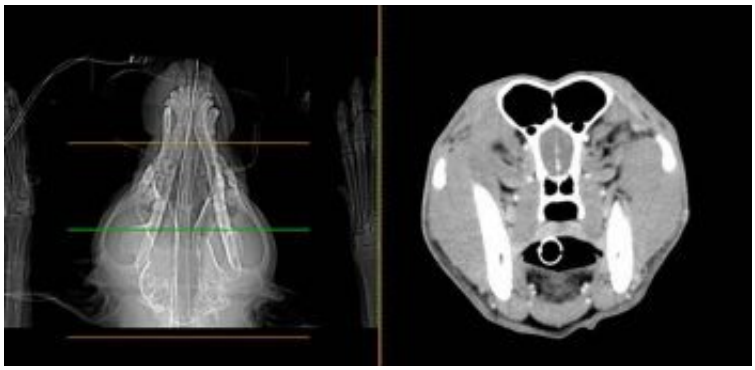

Figure 9. Examples of CT scout images. **9a** (left) is the scout sequence of the head. The orange lines represent the rostral and caudal extent of the CT scan and the green line represents the location of the CT slice displayed in **9b**.

A number of different scan modes are available for imaging. Scout scans are performed at the start of every CT study and are relatively low dose. This mode allows the user to define the scan region (**Figure 9**), as well as determine the amount of gantry tilt, if required, following which a sequential or helical scan can be performed[5].

Sequential scan

A sequential scan involves sequential scanning of single slices. This was mainly used before helical scanning was made available, as it was time-consuming to move the patient into position between scans[5].

Helical scan

As aforementioned, helical scans included continuous rotation of the x-ray tube and detector as the table was moved smoothly through the gantry. As this mode allows for rapid image acquisition, data can be acquired in a single breath-hold, and contrast-enhanced angiography studies can be performed[2]. This is the most common mode for “routine” veterinary CT.

Dynamic scan

Table 2. Effects of high mA and high kV

Outcome	High mA	High kV
Noise	↓	↓
Contrast resolution	↑	↓
Dose	↑	↑
Heat load	↑	↑

mA = milliamperes (current), kV = kilovoltage.

Table 2. Effects of high mA and high kV.

Dynamic scanning involves taking a series of images sequentially at the same location. It can be used to assess the insertion of ectopic ureters, how masses change following administration of contrast or for quantitative analysis of tissue perfusion[2]. Other uses include observation of physiological processes, such as the contractile motion of the heart, or pathological processes, such as shunts[5].

Image parameter selection

Current and kilovoltage

Current (milliamperes; mA) usually ranges from 50mA to 400mA, and can be selected individually or as part of presets. Higher mA settings will help reduce noise, while lower settings increase the amount of noise. If a small slice thickness is used, an increase in noise will occur, hence, mA should be increased to help counteract this problem.

Kilovoltage (kV) settings are usually set at 80kV, 100kV, 120kV or 140kV. For smaller patients, lower settings should be used. However, with lower kV settings, mA should be increased to maintain noise levels. For large patients, kV settings should not be too low, as it will result in lower

x-ray penetration, and may lead to decreased contrast resolution. **Table 2** summarises these effects.

Both current and kilovoltage add to the x-ray tube heat load. Therefore, limits exist as to how high both can be used. If higher doses are required, it is better to increase the mA settings rather than the kV settings[7].

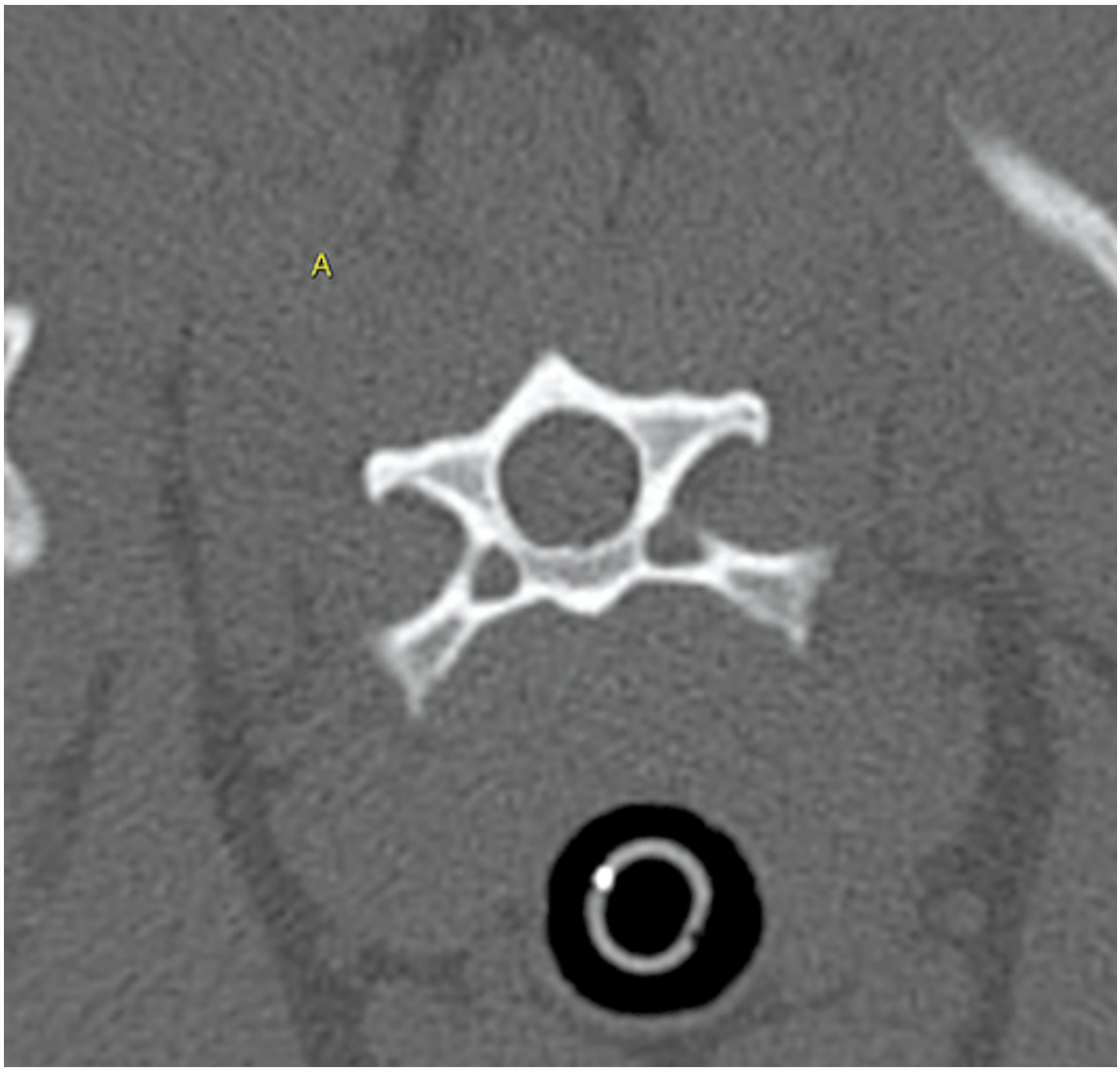

Figure 10a. This shows an optimal display field.

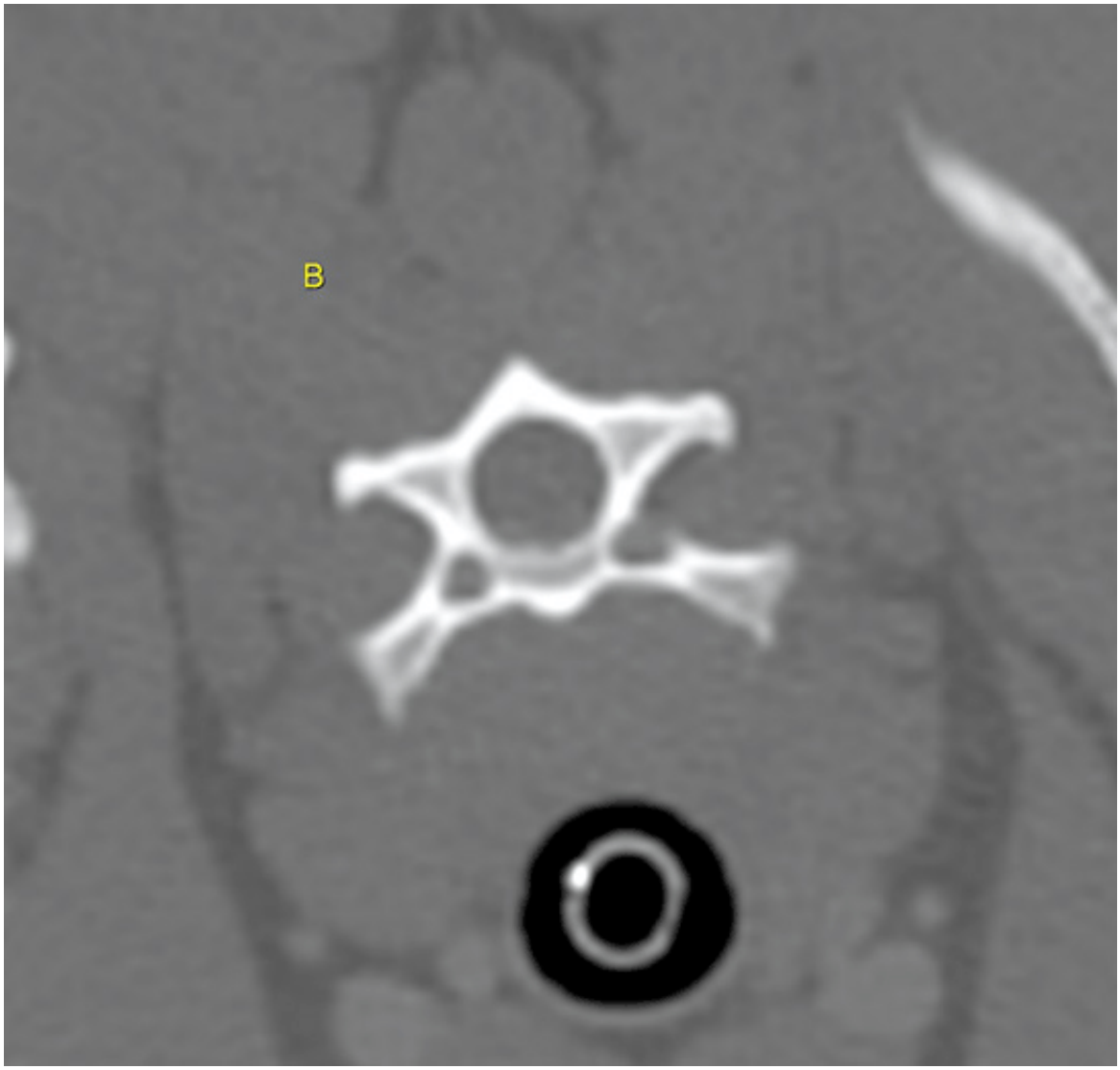

Figure 10b. A display field of view that was too large when the CT study was obtained. Note the difference in resolution of the vertebral bony detail in 10b compared with 10a.

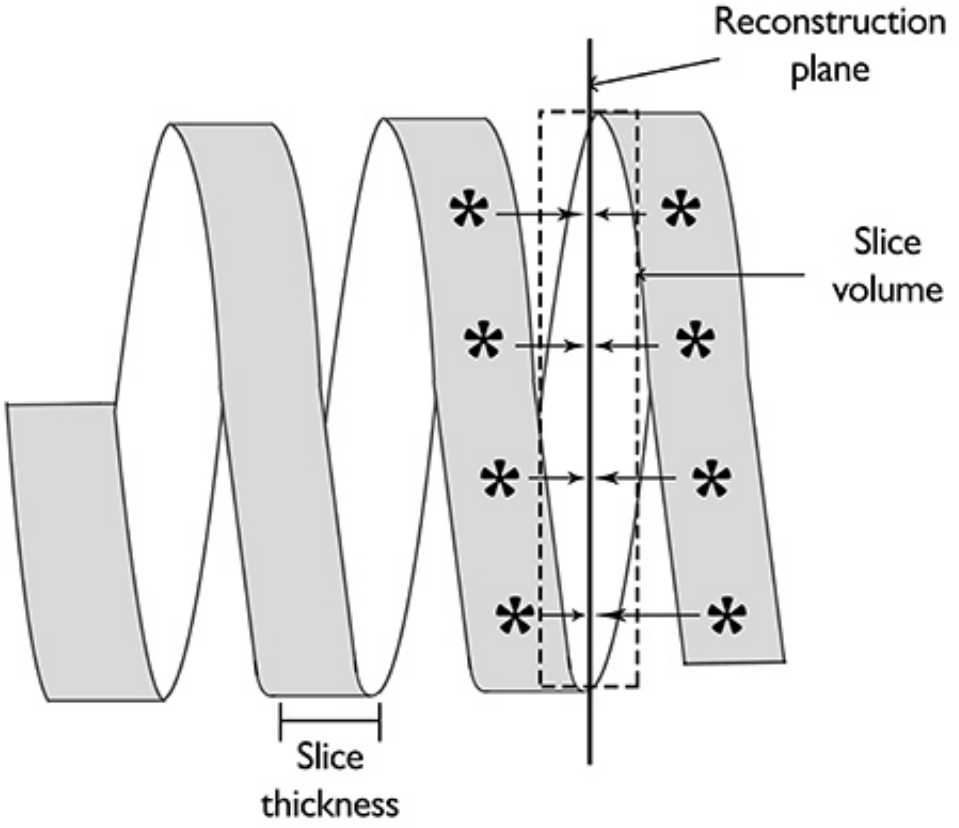

Figure 11. Data at similar locations along the helix are interpolated to form a 360° data set along the reconstruction plane, which is reconstructed to form an axial slice.

Field of views

When the x-ray fan beam hits detectors on the opposite side of the gantry, it results in a wedge-shaped area exposed to radiation. The scan field of view is thus the area of the gantry of circularly overlapping wedges. It should always be selected to be larger than the maximum diameter of the patient to avoid out-of-field artefacts.

The display field of view is the area in the scan field of view from which the image is reconstructed. It should be kept as small as possible to maximise image resolution (**Figure 10**)[7].

Thickness, interval and helical pitch

Slice thickness has an inverse relation to image noise and resolution. In other words, thin slices result in sharp, but noisy, images. Having thin slices also leads to prolonged scan times and increased heat loads, so it may not be possible to choose thin slices to scan a large area.

On the other hand, thick slices may not be able to detect things smaller than the slice width. For example, lung nodules may be missed if they are smaller than the slice width; they will still be visible, but may be blurred on the image. Thus, an initial slice width of 3mm to 5mm is recommended for screening metastatic lung disease and, if required, a short thin-slice series can be performed as a follow-up[7].

Slice interval is only applicable for non-helical modes and is the interval between CT slices. Most scanners will automatically input a slice interval equal to the slice width, to ensure a continuous image. However, this is limited by the x-ray tube heat capacity. One way around this is to acquire a small series of continuous slices, with gaps in between. This can be used for the scanning of intervertebral disc disease, whereby gaps can be left over the vertebral bodies[7].

For single-slice CT, pitch is described as the relationship between the distance the table moves and the slice thickness in one 360° rotation. For example, if the slice thickness is 10mm, and the table moves 10mm in one rotation, the pitch is 1. For multislice CT, pitch can be described as the relationship between the distance the table moves and either the width of all detectors combined (collimator pitch) or the width of each detector (detector pitch; **Figure 11**).

Existing data at similar locations along the helix are mathematically interpolated to form a data set, which is then reconstructed to form an image. The higher the pitch, the more mathematical interpolation inaccuracies and the more blurred the image[7]. A pitch of less than one would result in overlapping data and higher x-ray doses, but produce sharper images.

On the other hand, a pitch of more than one results in lower x-ray doses and faster scan times, but leads to gaps in exposed areas and a blurrier image[4]. For most clinical studies, a pitch of 1 to 1.5 is used[8].

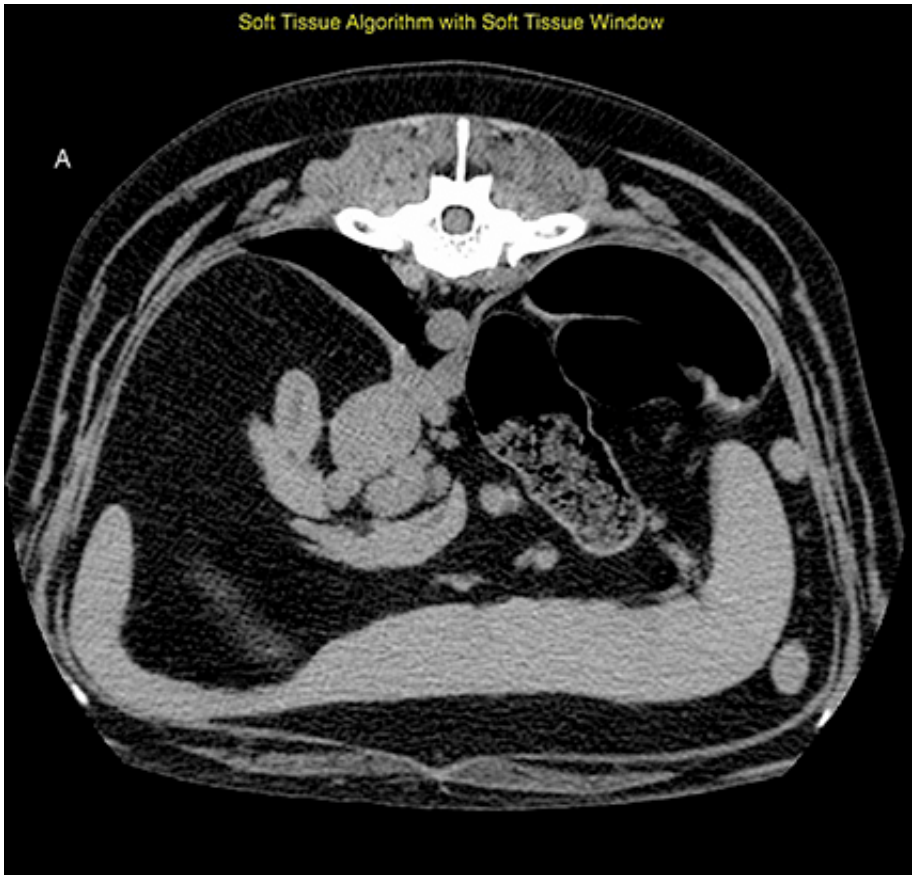

Figure 12a. CT images showing the difference between soft tissue and bone algorithms. 12a is a soft tissue algorithm with a soft tissue window applied, and B is a bone algorithm with a bone algorithm applied. Note in A the soft tissues have different shades of grey and are easier to evaluate than in 12b. Whereas in 12b, bony detail is visible of the vertebra and proximal ribs compared to 12a.

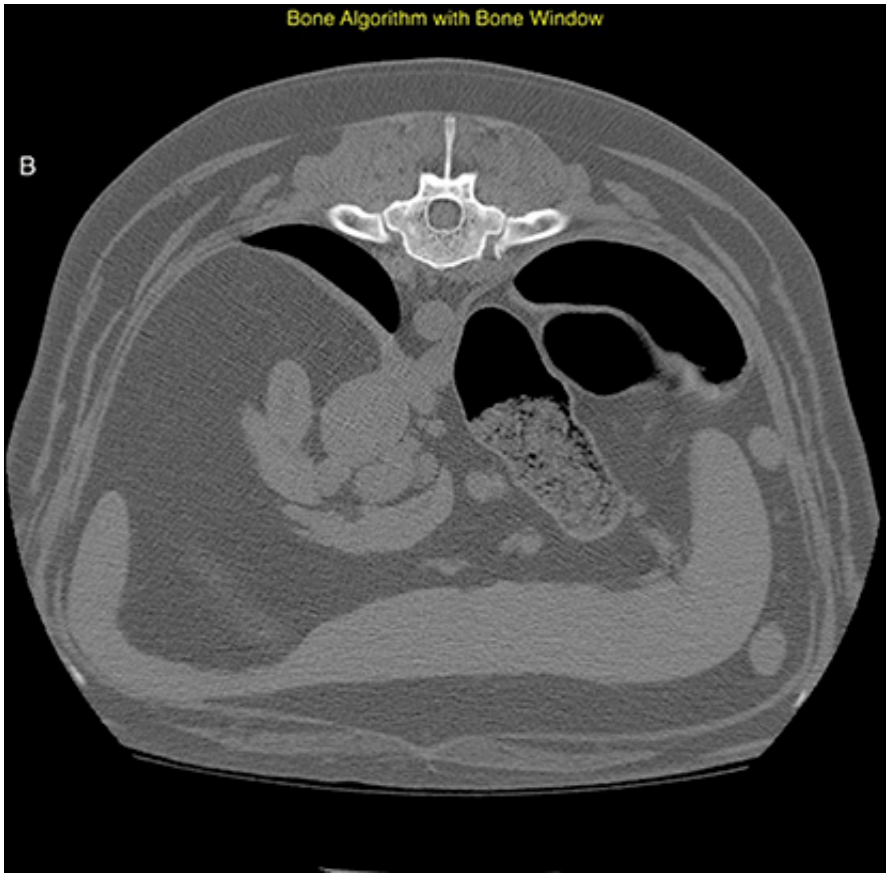

Figure 12b. CT images showing the difference between soft tissue and bone algorithms. 12a is a soft tissue algorithm with a soft tissue window applied, and B is a bone algorithm with a bone algorithm applied. Note in A the soft tissues have different shades of grey and are easier to evaluate than in 12b. Whereas in 12b, bony detail is visible of the vertebra and proximal ribs compared to 12a.

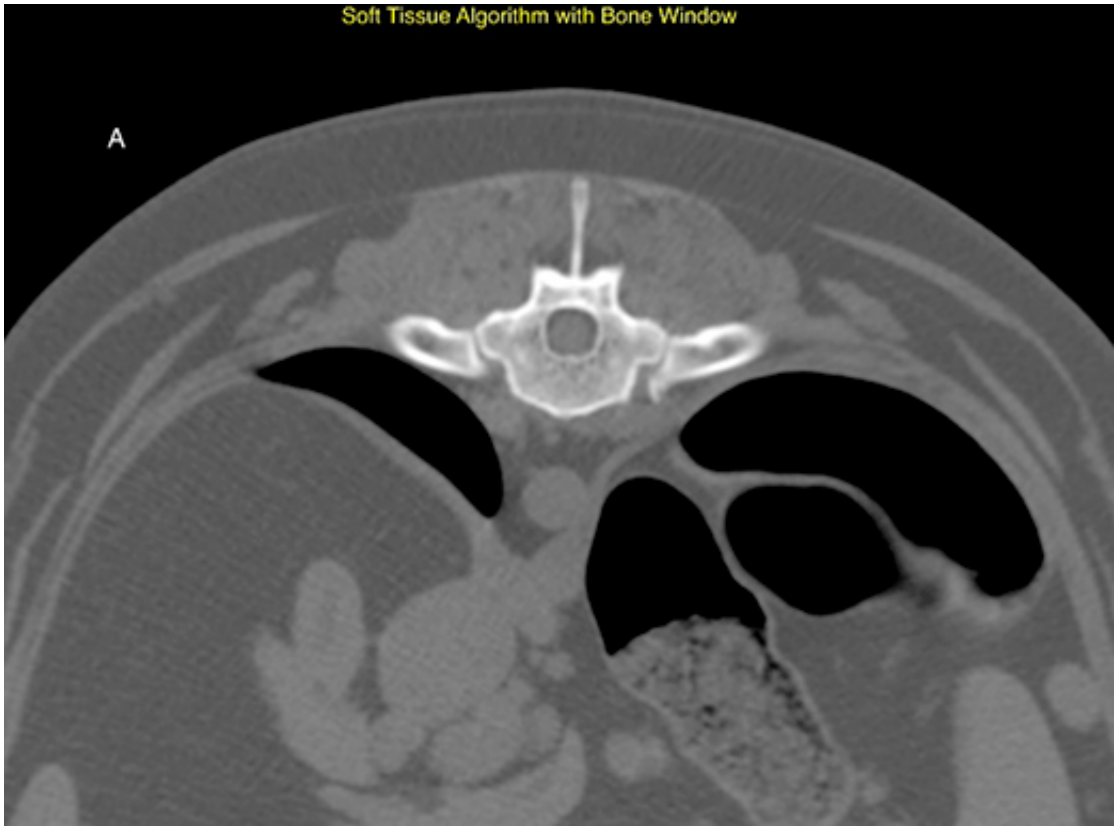

Figure 13a. CT images showing the difference between soft tissue and bone algorithms, with a bone window applied. 13a is a soft tissue algorithm with a bone window applied; note the blurry margins of the bone and loss of visualisation of the trabecular pattern.

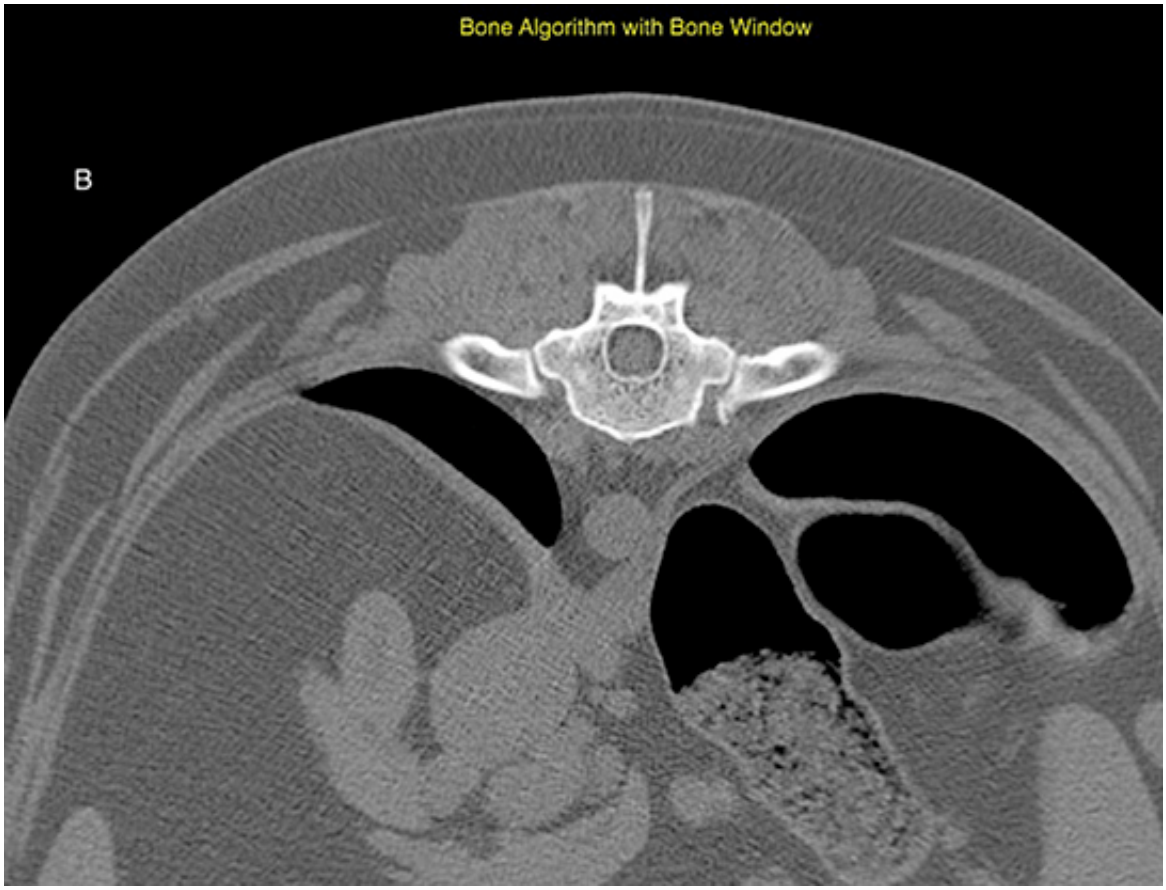

Figure 13b. CT images showing the difference between soft tissue and bone algorithms, with a bone window applied. 13a is a soft tissue algorithm with a bone window applied; note the blurry margins of the bone and loss of visualisation of the trabecular pattern.

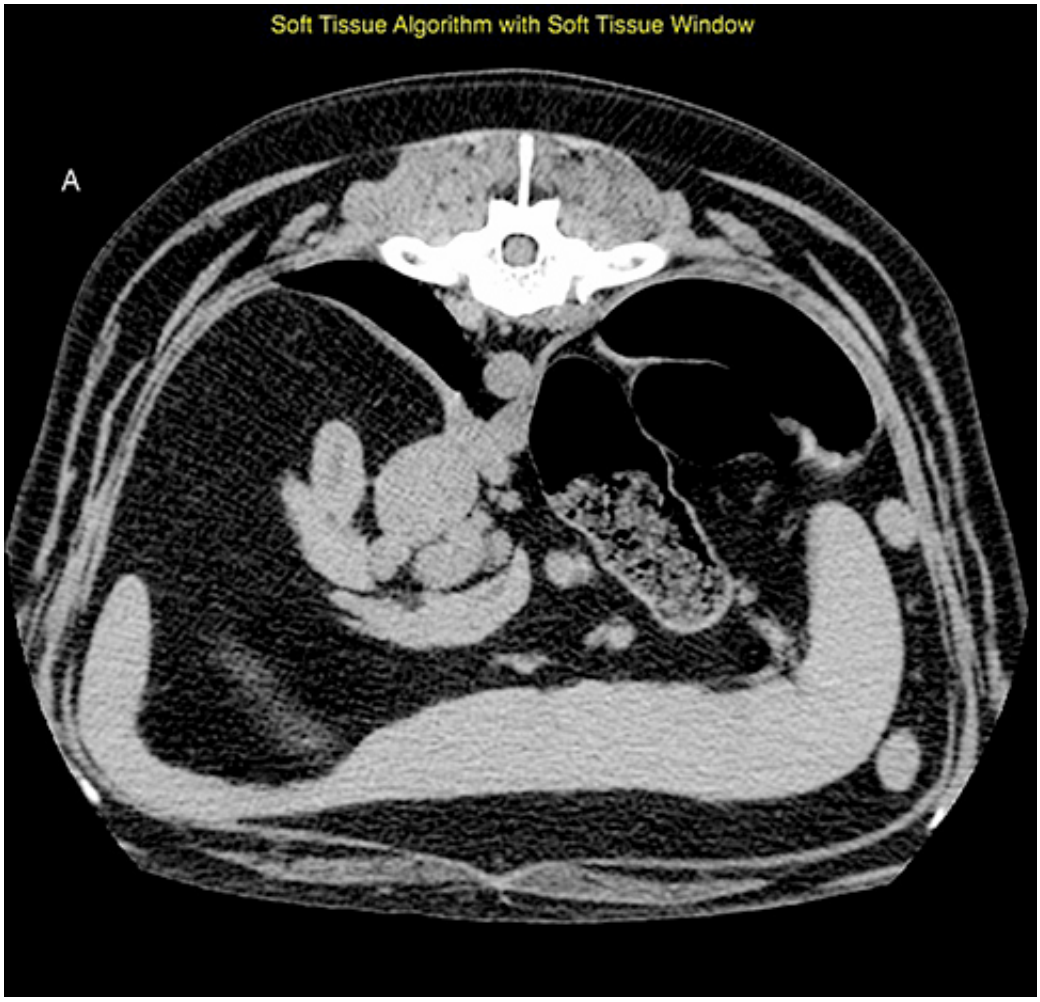

Figure 14a. CT images showing the difference between soft tissue and bone algorithms, with a soft tissue window applied. 14a is a soft tissue algorithm with a soft tissue window applied; note the smooth, well-defined appearance of the soft tissue abdominal organs. 14b is a bone algorithm with a soft tissue window applied. Note the grainy appearance of the abdominal organs and the lack of detail/differentiation between the organs.

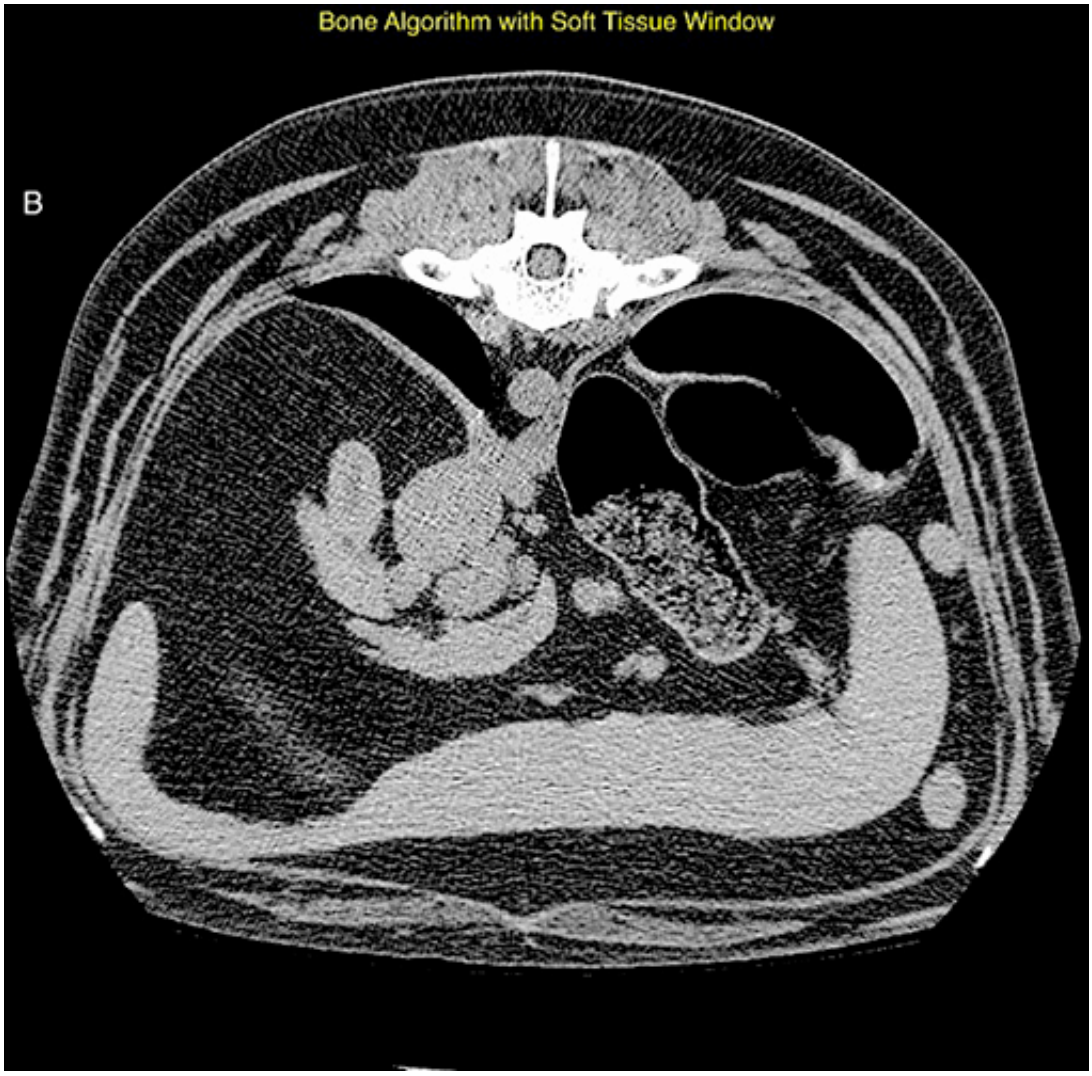

Figure 14b. CT images showing the difference between soft tissue and bone algorithms, with a soft tissue window applied. 14a is a soft tissue algorithm with a soft tissue window applied; note the smooth, well-defined appearance of the soft tissue abdominal organs. 14b is a bone algorithm with a soft tissue window applied. Note the grainy appearance of the abdominal organs and the lack of detail/differentiation between the organs.

Reconstruction filters

As mentioned earlier, filtered back projections are required for image reconstruction. Back projections alone result in blurry images, but the application of a mathematical filter function helps with this. Note that the term filter is interchangeable with the term algorithm.

A standard thorax and abdomen CT study will usually be reformatted in soft tissue, bone and lung algorithms.

“Bone filters” are used when structures of high contrast are imaged and high resolution is required so bone and tissue interfaces are sharp. However, a drawback of this is there is more noise.

“Soft tissue filters” are used when structures have less contrast, and reduced noise is desired, for example, to distinguish lesions in soft tissue. Although resolution is lower, the trade off for reduced noise is acceptable[4].

It is important to view the CT study with appropriate filters applied to get the most information out of the study.

Figure 12 illustrates the difference between soft tissue and bone algorithms. Once a mathematical algorithm has been applied, however, a window cannot be applied to change the type of algorithm. For example, if a bone algorithm is used, a soft tissue window cannot be applied to make it look like a soft tissue window. These are illustrated in **Figures 13 and 14**.

References

1. Thrall DE and Widmer WR (2013). Radiation protection and physics of diagnostic radiology. In Thrall DE (ed), *Textbook of Veterinary Diagnostic Radiology* (6th edn), Saunders Elsevier, St Louis: 2-21.
2. Goldman LW (2007). Principles of CT and CT technology, *Journal of Nuclear Medicine Technology* **35**(3): 115-128.
3. D’Anjou M-A (2013). Principles of computed tomography and magnetic resonance imaging. In Thrall DE (ed), *Textbook of Veterinary Diagnostic Radiology* (6th edn), Saunders Elsevier, St Louis: 50-73.
4. Dennis MJ (2010). Computed tomography. In *Encyclopedia of Medical Devices and Instrumentation*, John Wiley and Sons, New York: 230-258.
5. Saunders J and Ohlerth S (2011). CT physics and instrumentation – mechanical design. In Schwarz T and Saunders J (eds), *Veterinary Computed Tomography* (1st edn), John Wiley and Sons, West Sussex: 1-8.
6. Goldman LW (2008). Principles of CT: multislice CT, *Journal of Nuclear Medicine Technology* **36**(2): 57-68; quiz: 75-76.
7. Schwarz T and O’Brien R (2011). CT acquisition principles. In Schwarz T and Saunders J (eds), *Veterinary Computed Tomography* (1st edn), John Wiley and Sons, West Sussex: 9-28.
8. Saini S (2004). Multi-detector row CT: principles and practice for abdominal applications, *Radiology* **233**(2): 323-327.